The 178th ISIJ Meeting

Date

September 11 to 13, 2019

Venue

Okayama University, Tsushima Campus
2-1-1 Tsushima-naka, Kita-ku, Okayama 700-8530

Access (Source: Homepage of Okayama University)

1.Access from Okayama Airport:
1)Limousine Bus：
Limousine bus services are available from the airport to Okayama station (JPY760).

2)Taxi:
It costs approximately JPY5,000 from the airport to the Tsushima Campus.

2.Access from Okayama Station:
1)Taxi:
We recommend that you take a taxi from the station. There are several taxis waiting at both the east and west exits. The taxi fare to the Tsushima Campus is approximately JPY1,500. It is about 7 minutes from Okayama Station.

2)Bus:
There are frequent bus services from Okayama station.The bus fare is JPY 200. At JR Okayama Station West Exit Bus Terminal, take Okaden Bus for "Okayama rika daigaku" and get off at "Okadai nishimon".

3)Foot:
It is about 30 minutes from the Okayama station west exit.

For more information, please see the following website.
http://www.okayama-u.ac.jp/eng/access_maps/index.html

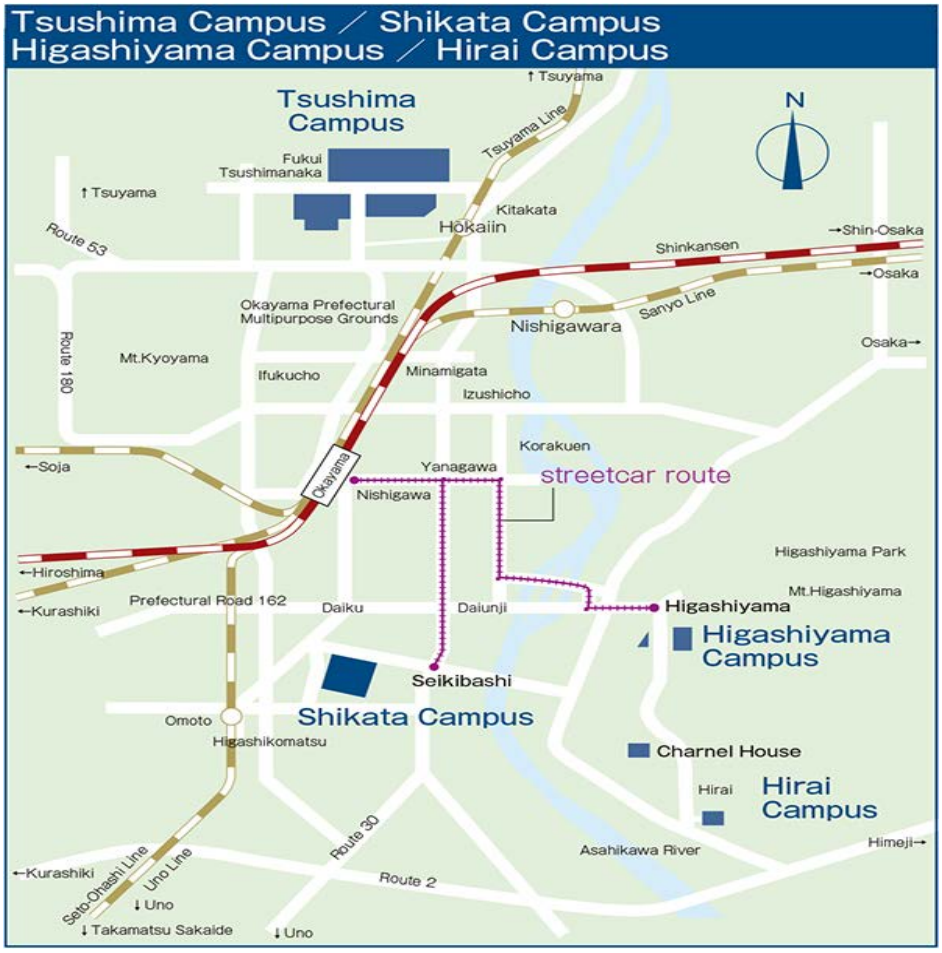

Banquet

1.Date: September 11, 2019 18:30～20:30

2.Vanue: Purity MAKIBI, Peacock room (2nd Fl.)
2-6-41 Shimoishii, Kita-ku, Okayama 700-0907
http://www.makibi.jp/

3.Fee: 8,000yen

Campus map

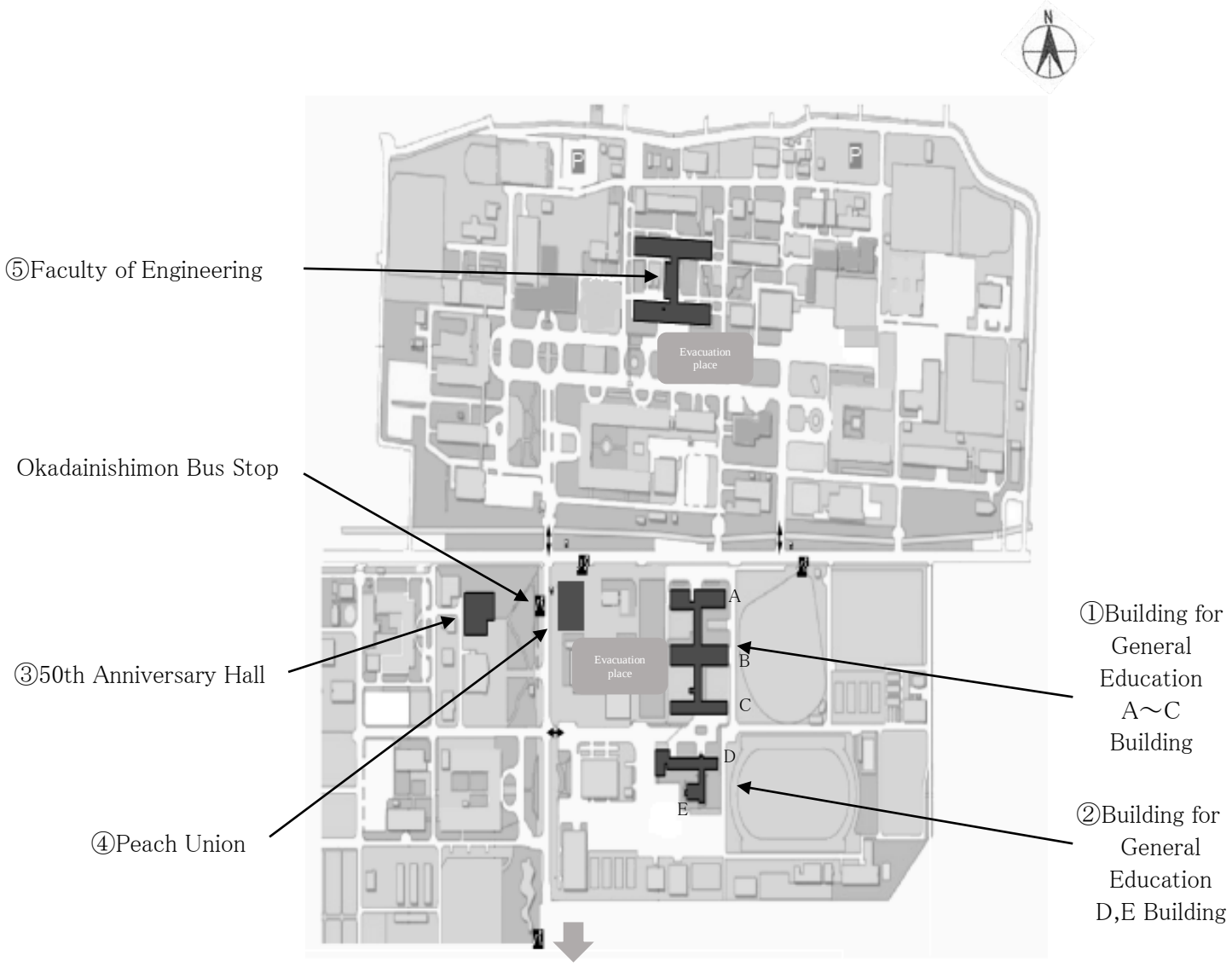

①A～C Building for General Education: ISIJ Reception Desk(2nd Fl.),
Session Room 1～14, 17(1st Fl.～4th Fl.), Secretariat (2nd Fl.)
②D,E Building for General Education: Session Room 15, 16(1st Fl.)
③50th Anniversary Hall: Poster Session for Students(2nd Fl.)
④Peach Union: ISIJ Beer Party (3rd Fl.), Cafeteria(2nd Fl.～3rd Fl.), Shop(1st Fl.)
⑤Faculty of Engineering Building No.1: The Japan Institute of Metals and Material's Session Room

Okayama University is a completely non-smoking environment.

A～C Building for General Education

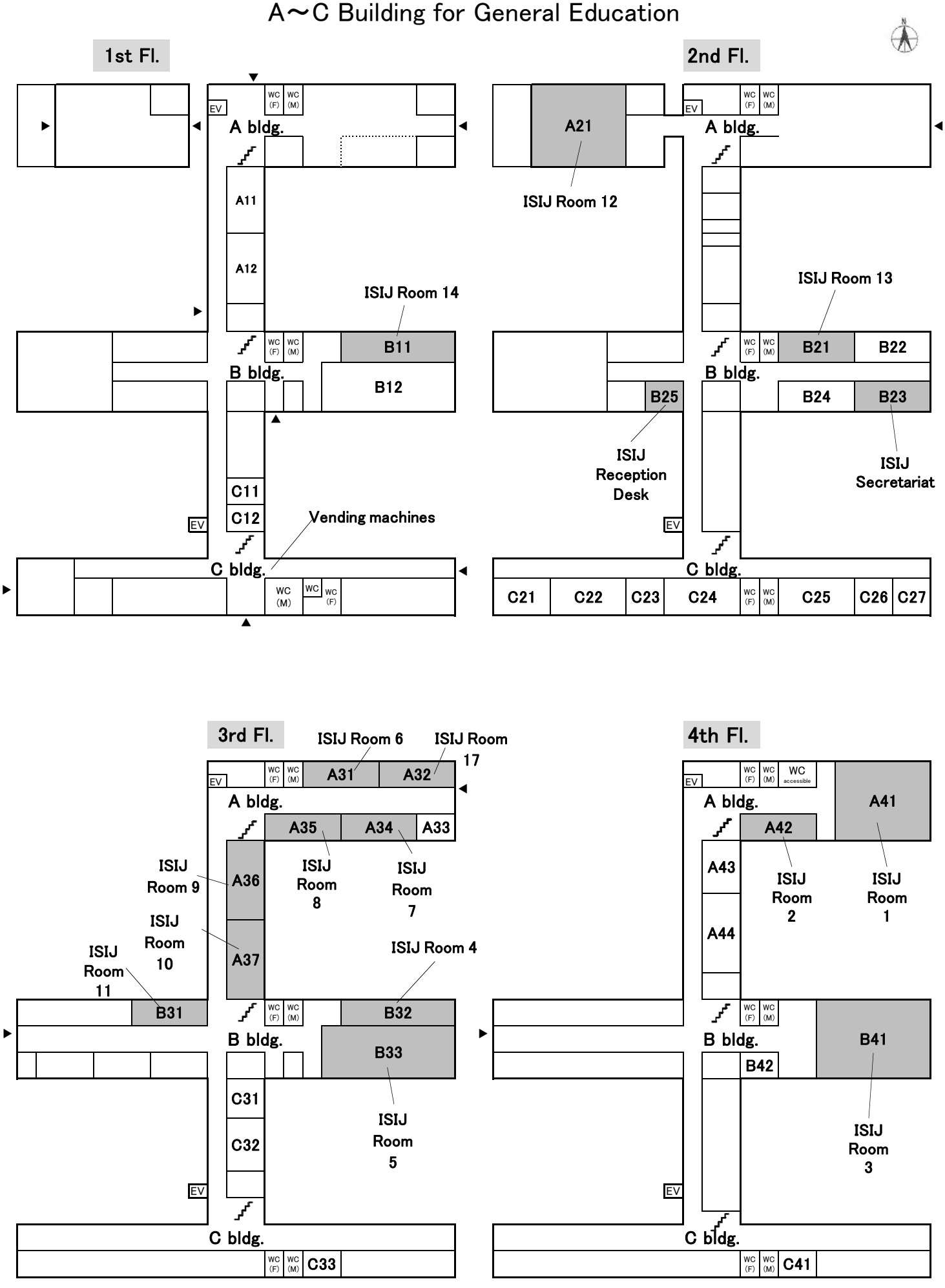

D,E Building for General Education

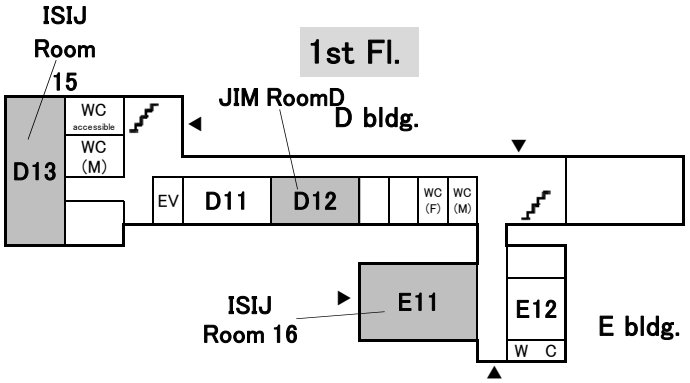

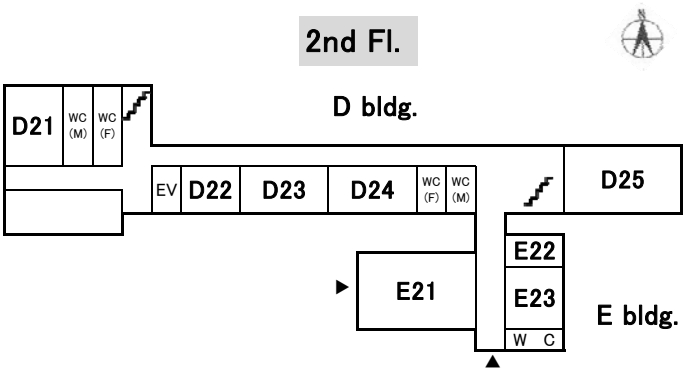

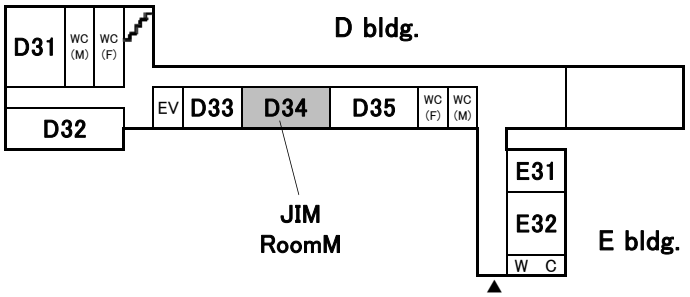

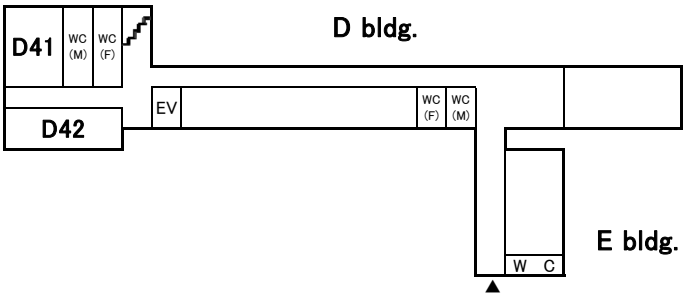

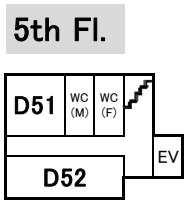

The timetable the 178th ISIJ Meeting
(September 11–13, 2019 at Okayama University, Tsushima Campus)

Session Room	Sept. 11 (Wed.)		Sept. 12 (Thu.)		Sept. 13 (Fri.)	
	AM	PM	AM	PM	AM	PM
Session Room 1 Bldg. for General Education 4th fl. A41	Contribution of steelmaking technology for the sustainable development in Asia [Int.-1–Int.-11] (9:30–15:50)		Thermodynamics/ Transport phenomena [23–30] (9:00–11:50)	Converter and electric furnace/Secondary refining [31–38] (13:00–15:50)	Control of solidified structure of steelmaking slag for suppression of elution of alkali (9:00–11:50) [Charge-free]	---
Session Room 2 Bldg. for General Education 4th fl. A42	Novel processing/Electromagnetic processing of materials [1–7] (9:30–12:00)	Analysis and quantification of segregation and defect during solidification (13:00–16:25) [Charge-free]	Advanced utilization of by-materials/Eco-process and iron making [99–107] (9:00–12:10)	---	---	---
Session Room 3 Bldg. for General Education 4th fl. B41	Cohesive zone in blast furnace 1・2 [8–14] (9:20–11:50)	Current state and challenges for future advancement of instrumentation technology for ironmaking process (13:00–17:20) [Charge-free]	Reactions and operation estimation of blast furnace/ Raceway in blast furnace [39–45] (9:00–11:30)	Current situations and issues on characterization of multi-component calcium ferrite aiming for production of high-performance iron ore sinters [D1–D5] (13:00–16:10)	Young engineer session of iron making/Sintering process 1 [59–65] (9:00–11:30)	Sintering process 2/ Analysis of sinter [66–73] (13:00–15:50)
Session Room4 Bldg. for General Education 3rd fl. B32	Effective utilization of resources 1・2 [15–22] (9:10–12:00)	Evaluation of social value of material in the value chain (13:00–16:50) [Charge-free]	Young engineer session of coke-making 1・2 [46–52] (9:00–11:30)	Young engineer session of coke-making 3/Coke [53–58] (13:00–15:10)	Inclusion [74–77] (10:00–11:20)	Slag and dust treatment [78–82] (13:00–14:40)
Session Room 5 Bldg. for General Education 3rd fl. B33	---	Carbon dioxide Capture-Less-Utilize (CCLU) process without CO_2 separation and recovery (13:00–17:00) [Charge-free]	Technology and history of the iron and related industries in Chugoku area Japan (10:00–17:00) [General: 2,000yen, Student: 1,000yen]		Solidification and structure control/Continuous casting and solidification 1 [83–91] (9:00–12:10)	Continuous casting and solidification 2・3 [92–98] (13:10–15:40)
Session Room 6 Bldg. for General Education 3rd fl. A31	Advanced abnormality diagnoses based on area sensing technologies [D6–D10] (9:20–12:00)	---	Instrumentation 1・2 [108–114] (9:00–11:30)	Control and system [115–118] (12:30–13:50) Human-system shared control realizing high efficient and stable rolling [D11–D15] (14:00–16:35)	---	---
Session Room 7 Bldg. for General Education 3rd fl. A34	Modeling of various phenomena in metal forming and its application 1・2 [119–125] (9:20–11:50)	Current research and development of width control in hot rolling [D16–D20] (13:00–16:50)	Symposium on formation and nano-level analysis of excellent hot-dip Zn coating layer (9:00–16:35) [Charge-free]		Scale and cooling/Cooling [152–158] (9:20–11:50)	Hot rolling/ Fundamental tribological studies on manufacturing processes [159–168] (13:00–16:30)
Session Room 8 Bldg. for General Education 3rd fl. A35	---	Reliability evaluation of steel weld 1・2/Control technology for free cutting–13 [126–135] (13:00–16:40)	The technical session by young engineers of hot rolling 1・2 [136–141] (9:30–11:40)	Young engineer's latest researches on tubes and pipes Ⅱ–1・2/Advances in processing of powders and powder metallurgy [142–151] (13:00–16:40)	---	---
Session Room 9 Bldg. for General Education 3rd fl. A36	Modeling and simulation 1・2 [169–176] (9:10–12:00)	Frontier of quantum beam analysis for metallic microstructures Ⅱ (13:00–16:55) [Charge-free]	Stainless steels 1 [212–215] (10:30–11:50)	Stainless steels 2・3 [216–223] (13:30–16:20)	Fatigue property/ Toughness and ductility [270–277] (9:00–11:50)	---
Session Room 10 Bldg. for General Education 3rd fl. A37	Fatigue damage on surface hardened alloy steels for machine structural use, 2nd (9:20–16:00) [Charge-free]		Strength and deformation behavior 1・2 [224–231] (9:00–11:50)	Strength and deformation behavior 3・4・5 [232–241] (13:00–16:40)	Hot-dip coating [278–282] (10:20–12:00)	Chemical property [283–286] (13:00–14:20)
Session Room 11 Bldg. for General Education 3rd fl. B31	Plate and machine structural steel [177–179] (11:00–12:00)	---	Electrical steel 1・2 [242–248] (9:10–11:40)	Recrystallization and grain growth 1・2 [249–256] (13:30–16:20)	---	---
Session Room 12 Bldg. for General Education 2nd fl. A21	Phase transformation/ Aging and precipitation [180–186] (9:10–11:40)	Microstructure formation 1・2 [187–193] (13:20–15:50)	Ferritic heat resistant steel 1・2 [257–264] (9:00–11:50)	Austenitic heat resistant steel and heat resistant alloy [265–269] (13:30–15:10)	Inhomogenous deformation and mechanical properties of steels (9:00–15:10) [Charge-free]	
Session Room 13 Bldg. for General Education 2nd fl. B21	---	ISIJ and JIM joint session Titanium and its alloys 1・2 [J1–J10] (13:00–16:30)	---	---	ISIJ and JIM joint session Titanium and its alloys 3・4 [J11–J18] (9:00–11:50)	---
Session Room 14 Bldg. for General Education 1st fl. B11	---	ISIJ and JIM joint session Materials science of martensitic and bainitic transformations and its applications 1 [J28–J31] (13:10–14:30)	ISIJ and JIM joint session Materials science of martensitic and bainitic transformations and its applications 2・3・4・5・6 [J32–J50] (9:00–17:00)		ISIJ and JIM joint session Materials science of martensitic and bainitic transformations and its applications 7・8 [J51–J58] (9:00–11:50)	---
Session Room 15 Bldg. for General Education 1st fl. D13	---	High-strengthening theory in high-temperature materials Ⅱ (13:00–17:10) [Charge-free]	Recent advancement of studies on phase transformation and precipitation in Titanium alloys (10:00–15:45) [Charge-free]		---	---
Session Room 16 Bldg. for General Education 1st fl. E11	Hydrogen embrittlement 1・2 [194–199] (9:40–11:50)	Hydrogen embrittlement 3・4・5 [200–211] (13:00–17:20)	Mechanism of fracture and practical issues in hydrogen embrittlement (9:00–16:50) [2,000yen]		Hydrogen embrittlement 6・7 [287–293] (9:20–11:50)	Hydrogen embrittlement 8 [294–296] (13:00–14:00)
Session Room 17 Bldg. for General Education 3rd fl. A32	---	---	Surface and state analysis/ Crystal structure analysis [297–303] (9:10–11:40)	Fabrications of new functionalities of biofilm-covered and/or chemically treated slags and their analyses (13:00–16:25) [Charge-free]	Elemental analysis 1 [304–307] (10:30–11:50)	Board Meeting of Process Evaluation and Material Characterization (13:00–14:00) [Charge-free] Elemental analysis 2 [308–310] (14:10–15:10)
JIM Session Room D Bldg. for General Education 1st fl. D12	---	---	---	---	ISIJ and JIM joint session Ultrafine grained materials –fundamental aspects for ultrafine grained structures– 1・2・3 [J19–J27] (9:00–12:20)	---
JIM Session Room M Bldg. for General Education 3rd fl. D34	---	---	ISIJ and JIM joint session Physico-chemical properties of high temperature melts 1・2・3・4・5 [J59–J76] (9:00–17:20)		---	---
	Banquet (18:30–20:30 Purity MAKIBI 2nd fl. Peacock room) [8,000yen]		Poster Session for Students (12:00–16:00 50th Anniversary Hall) ISIJ Beer Party (17:30–19:00 Peach Union 3rd fl.) [1,000yen]			

[ ]: Lecture Number
( ): Lecture Time
: Symposium: Please ask to each of symposium room desks directly

Program of the 178th ISIJ Meeting (September 11-13, 2019)

Discussion Sessions

High Temperature Processes / Process Evaluation and Material Characterization

Lecture No. | Discussion Session | Title | Speaker | Page

Current situations and issues on characterization of multi-component calcium ferrite aiming for production of high-performance iron ore sinters

13:05-13:45
D1 Sintering technologies for high quality sintered ore at JFE Steel — T. Higuchi · · · 399

13:45-14:25
D2 Reduction behavior of silico-ferrite of calcium and aluminum under blast furnace condition — T. Murakami · · · 403

14:25-14:40
D3 withdraw

14:40-15:20
D4 Current state of multi-component phase diagram including SFCA phase — R. Murao · · · 405

15:20-16:00
D5 Structural study of multi-component calcium ferrite (SFCA) phase — K. Sugiyama · · · 409

Instrumentation, Control and System Engineering

Lecture No. | Discussion Session | Title | Speaker | Page

Advanced abnormality diagnoses based on area sensing technologies

9:20-9:30
D6 Intelligent abnormality diagnosis for steel works by using adaptive area sensing — H. Tamaki · · · 412

9:30-10:00
D7 Remote monitoring of conveyor belt using a mirror-drive active vision — I. Ishii · · · 413

10:00-10:30
D8 Small vibration measurement and rotating angle measurement of a conveyer belt using sampling moire camera — M. Fujigaki · · · 415

10:40-11:10
D9 Parameter dependent models for health diagnosis of equipments based on state, parameter and input estimation method — T. Asai · · · 418

11:10-11:40
D10 Unknown anomaly detection using hidden markov model and area sensing technology — I. Ono · · · 420

Instrumentation, Control and System Engineering / Processing for Quality Products

Lecture No. | Discussion Session | Title | Speaker | Page

Human-system shared control realizing high efficient and stable rolling

14:05-14:35
D11 Theories and characteristics of tandem srip rolling — F. Fujita · · · 424

14:35-15:05
D12 On simulator for cold tandem rolling control systems — O. Kaneko · · · 428

15:05-15:35
D13 (Invited Lecture) Mazda's vision for cars of the future — T. Tochioka · · · 432

15:35-16:05
D14 Taxonomy and examples of shared control — M. Itoh · · · 436

16:05-16:35
D15 Issues and prospects of shared control for tandem cold rolling — A. Kitamura · · · 438

Processing for Quality Products

Lecture No.
Discussion Session | Title | Speaker | Page

Current research and development of width control in hot rolling

13:05-13:45
D16 Strip width control technology for hot strip mill — S. Fukushima ・・・ 441

13:45-14:25
D17 The state and issues of width control for hot strip mills — M. Sano ・・・ 445

14:35-15:15
D18 Evaluation for deformed profile of Slab-End due to conditions of rolling and press reduction — Y. Nakamura ・・・ 449

15:15-15:55
D19 (Invited Lecture) Influence of sizing press condition on plan view pattern of sheet bar in hot strip mill — H. Goto ・・・ 453

15:55-16:35
D20 Introduction of recent slab sizing press — T. Kamoshita ・・・ 457

Program of the 178th ISIJ Meeting (September 11-13, 2019)

International Organized Sessions

High Temperature Processes
2019/9/11 Room1 (Bldg. for General Education 4th fl. A41)

Contribution of steelmaking technology for the sustainable development in Asia

Session Organizer: S. Kitamura [Tohoku Univ.]

9:30-9:35
Opening Remark: S. Kitamura [Tohoku Univ.]

Chair: S. Ueda [Tohoku Univ.]

9:35-10:00
Int.-1 (Invited Lecture) Experimental study on DRI production by both of composite carbon and gas reduction
Dong-A Univ. ○Y. Kang・S. Song ・・・ 458

10:00-10:25
Int.-2 New refining technologies for high-purity steel and minimization of steelmaking slag
JFE ○Y. Nakai・N. Kikuchi・Y. Kishimoto ・・・ 462

10:25-10:50
Int.-3 Solution models applied to estimate thermochemical properties of the $CaO\text{-}SiO_2\text{-}P_2O_5\text{-}Fe_xO$ dephosphorization slags at 1573K
Kyoto Univ. ○M. Hasegawa・K. Saito・Y. Oshima ・・・ 466

Chair: N. Saito [Kyushu Univ.]

11:05-11:30
Int.-4 (Invited Lecture) Effect of natural convection on formation and melting of shell around low melting point additives in steel
IIT Kanpur ○A. K. Singh・A. Arya ・・・ 470

11:30-11:55
Int.-5 Development of full utilization process of steelmaking slag
Nippon Steel ○T. Harada・M. Sakamoto・S. Kakimoto ・・・ 474

Chair: M. Hayashi [Tokyo Inst. Tech.]

13:00-13:25
Int.-6 Crystallization behavior of molten slags characterized under alternative current field
Kyushu Univ. ○N. Saito・K. Nakashima ・・・ 477

13:25-13:50
Int.-7 (Invited Lecture) Control of optimum argon shrouding practice - A water model study
IIT Bombay ○N. N. Viswanathan・N. B. Bharath・G. Kalaivani, JSW S.P. Jayaraj ・・・ 478

13:50-14:15
Int.-8 (Invited Lecture) The role of an upper slag phase and thermal in-homogeneity in melt on grade intermixing time in a tundish at constant throughput rate
IIT Kanpur ○D. Mazumdar・S. Chakraborty ・・・ 482

Chair: S. Kitamura [Tohoku Univ.]

14:30-14:55
Int.-9 (Invited Lecture) Key issues of molten steel initial solidification during the process of casting
Central South Univ. ○W. Wang・P. Lyu ・・・ 486

14:55-15:20
Int.-10 (Invited Lecture) Calcium cored wire injection for stable casting: An insight into fundamentals and economics
IIT Kharagpur ○G. G. Roy・B. Kumar ・・・ 489

15:20-15:45
Int.-11 MnS precipitation behavior around $MnO\text{-}SiO_2$ inclusion in Fe-Mn-Si-O-S alloy system at the solid-liquid equilibrium temperature
Tohoku Univ. ○J. Gamutan・T. Miki・T. Nagasaka ・・・ 493

15:45-15:50
Closing Remark: S. Kitamura [Tohoku Univ.]

Program of the 178th ISIJ Meeting (September 11-13, 2019)

High Temperature Processes

Lecture No. Plenary Session	Title	Speaker	Page
Novel processing			
1	Influence of ultrasonic vibration surface roughness on droplet shape	Y. Tanaka	497
2	Improvement of the performance of quasi-zeolite particles synthesized from fly-ash	T. Kozuka	498
3	Phase separation of slag using aggregation by magnetic field	M. Nagano	499
Electromagnetic processing of materials			
4	Influence of composition on heating and flow in molten V_2O_5-Na_2O under electromagnetic induction	N. Yoshikawa	500
5	Effect of copper rods' position in circular pipe on liquid tin flow under magnetic field imposition	S. Iimura	501
6	Velocity estimation for concentration boundary layer thickness decrease mechanism analysis under simultaneous imposition of current and magnetic field	G. Xu	502
7	Grain refinement mechanism of solidified structure by ultrasonic vibration under condition of flow suppression	N. Tabayashi	503
Cohesive zone in blast furnace 1			
8	An experimental approach to the softening and melting behavior of acid pellet with low-MgO sinter	M. Sun	504
9	Deformation behavior of a packed bed of softening particles	K. Baba	505
10	Gas clogging evaluation due to ore layer softening by eulerian-lagrangian method	S. Natsui	506
11	Trickle flow analysis considering liquid iron-molten slag-coke triple line by SPH	K. Tonya	507
Cohesive zone in blast furnace 2			
12	Modeling of ash particles behaviors during reaction of cokes	K. Teshima	508
13	Relocation of molten CaO-SiO_2-Al_2O_3-FeO droplet on surface of reducing agent	S. Ueda	509
14	Factors affecting static hold up of molten slag in coke-packed bed	Y. Lee	510
Effective utilization of resources 1			
15	(ISIJ Research Promotion Grant) Recycling of phosphorus from steel making slag with microalgae II	Y. Hoshikawa	511
16	Long term dissolution behavior of CaO-SiO_2-FeO_x glassy phase - $2CaOSiO_2$ coexisting slag in paddy field environment	S. Koizumi	512
17	Effect of moisture content on briquetting formability of steel mill dust	K. Maeda	513
18	The study on re-use technology of valuable metal-containing dust for RHF	Y. Jeong	514
Effective utilization of resources 2			
19	Segregation of reduced fine iron ore in powder particle fluidized bed	K. Fujino	515
20	Reduction mechanism of carbon-iron ore composite prepared using lignite	K. Sato	516
21	Removal of gangue in low-grade iron ore by hydrothermal treatment	Y. Mochizuki	517
22	Separation of phosphorus from Mn ore by selective reduction	X. Gao	518
Thermodynamics			
23	Oxygen partial pressure and basicity dependence on the solubility of CrO_x in CaO-SiO_2-CrO_x slag at low oxygen partial pressure	C. Kato	519
24	Determination of CrO_X activity in CaO-SiO_2-CrO_X slag under reducing condition	Z. Li	520
25	The thermodynamic property of B in molten Si-Cu-Sn alloy	T. Mizutani	521
26	Phase relation of Fe-Mn-S and Fe-Cr-S system	Y. Lu	522
Transport phenomena			
27	(ISIJ Research Promotion Grant) In-situ observation of bubble at the molten salt / Sn interface by controlling applied potential	H. Konishi	523
28	Trial for in-situ interface observation of desulfurization reaction in molten pig iron-lime system	H. Esaka	524
29	A kinetic model of mass transfer and chemical reactions at a steel/slag interface under effect of interfacial tensions	P. Ni	525
30	Effects of top and bottom blowing conditions on spitting generation phenomena	S. Sato	526
Converter and electric furnace			
31	Computational fluid dynamics simulation on tapping operation of converter	Y. Higuchi	527
32	Nitrogen pickup during tapping of liquid steel from induction furnace to ladle	A. Okayama	528
33	Effective combined blowing technique with slag splashing	L. Yang	529
34	withdraw		

Program of the 178th ISIJ Meeting (September 11-13, 2019)

Secondary refining

35 (ISIJ Research Promotion Grant) Mass transfer analysis of gas-liquid interface in a gas stirred vessel — H. Arai · · · 530
36 Investigation on bubble fragmentation and inclusion behavior in a simplified model of RH degasser — T. Yamamoto · · · 531
37 Examination of control of peeling slag protection layer at MgO-C brick — H. Yano · · · 532
38 Investigation of the steel ladle refractories for safety lining to avoid the molten steel and slag leaking — S. Takahashi · · · 533

Reactions and operation estimation of blast furnace

39 withdraw
40 Prediction of oxygen blast furnace reductants ratio restricted by operating conditions — K. Nakamura · · · 534
41 Effect of highly reactive burden on blast furnace shaft reaction — Y. Park · · · 535
42 Non-equilibrium state of boudour reaction — K. Nagata · · · 536

Raceway in blast furnace

43 Effect of the characteristics of pulverized coal on blast furnace operation — D. Seo · · · 537
44 Simulation of gas-particle motion around raceway in cold model — S. Taya · · · 538
45 Raceway formation and coke combustion CFD simulation — J. De Castro · · · 539

Young engineer session of coke-making 1

46 Inhibitory influence of carbon material on dilatation of coking coal — N. Kawadai · · · 540
47 Effect of coal particle arrangement on coke strength after carbonization — H. Noma · · · 541
48 Stress simulation analysis of high strength coke using X-ray CT image — T. Tomono · · · 542
49 The analysis of coke micro structure using X-CT — M. Kitao · · · 543

Young engineer session of coke-making 2

50 Development of environmentally-friendly processing technology/Development of ferrocoke technology — H. Fujimoto · · · 544
51 Ferro-coke production technologies using low-grade raw materials — M. Nagayama · · · 545
52 Mixing analysis of ferro-coke materials — S. Hiroike · · · 546

Young engineer session of coke-making 3

53 Stabilization of blast furnace operation by quality improvement of yard coke — S. Aikawa · · · 547
54 Enhancement of efficiency in hot repair for coke oven battery — R. Urakawa · · · 548
55 Evaluation of door-opening brick relaying for Nagoya No2 coke oven — D. Minori · · · 549

Coke

56 Study on the effect of stockline level on coke distribution in CDQ by DEM — Z. Fan · · · 550
57 Study on the effect of bell angle on coke distribution in CDQ by DEM — Z. Fan · · · 551
58 Combustion behavior of coke gas in coke oven emission facilities — T. Kawashima · · · 552

Young engineer session of iron making

59 Improvement of coke ratio at Kashima works — T. Nakamura · · · 553
60 Technology to control agglomeration characteristics on using fine concentrate ore for sinter process — M. Taniguchi · · · 554
61 Effect of iron ore properties on pore structure of iron ore sinter — R. Kosugi · · · 555
62 Improvement of heat recovery efficiency by installation of water-seal cooler — M. Ishikawa · · · 556

Sintering process 1

63 Methodology for continuous pelletization of carbon-cored, double-layered green pellet — K. Iwase · · · 557
64 withdraw
65 Time variation of temperature distribution in sinter beds and its dependence on radial position (1) — K. Taira · · · 558

Sintering process 2

66 In-situ temperature monitoring of sinter beds at high spatial resolution (3) — K. Taira · · · 559
67 Effect of oxygen partial pressure on the oxidation behavior of iron bearing materials — D. Maruoka · · · 560
68 Evaluation of density distribution in sintering bed by X-ray CT — K. Hara · · · 561
69 Influence of chlorine of fine particulate matters emitted from iron ore sintering process — Z. Ma · · · 562

Analysis of sinter

70 Effects of MgO addition and source on formation of acicular silico-ferrite of calcium and aluminum (SFCA) in sinter ore — H. Ochi · · · 563

71 Effect of $2CaOSiO_2$ addition on microstructures of iron ore sinters — D. Zhou · · · 564

72 Effect of gangue minerals on strength and texture of fine powder granule — S. Nakamura · · · 565

73 AE measurement system of iron ore sinter in conjunction with micro Vickers — M. Mizutani · · · 566

Inclusion

74 In-situ observation model for inclusion removal with bubble floatation by using Antibubble — Y. Hirai · · · 567

75 Microscopic observation of the interface reaction phase between cermet tool and oxide using three-dimensional atom probe — Y. Hosono · · · 568

76 A discussion on microstructural differences in the heat affected zones of EH36 shipbuilding steels with Mg and Zr additions — X. Zou · · · 569

77 Three-dimensional observation of typical inclusions in steel by X-ray micro-CT — Z. Shang · · · 570

Slag and dust treatment

78 Behavior of slag crystallization in continuously blast furnace slag solidification process — Y. Ta · · · 571

79 Reduction behavior of EAF slag containing Cr_2O_3 and MnO — H. Fukaya · · · 572

80 Surface observation of calcium-silicate mineral phases after their dissolution into water — F. Ruan · · · 573

81 Thermodynamic study for the effect of organic acid addition on elution of glassy phase in steelmaking slag — T. Kawasaki · · · 574

82 Reaction behavior of $ZnFe_2O_4$ in a $MgCl_2$-based molten salt — Y. Nishioka · · · 575

Solidification and structure control

83 Crystallographic orientation before and after the massive-like transformation in Fe-18Cr-Ni alloy — K. Ichida · · · 576

84 Investigation of composition range for selection of the massive-like transformation in Fe-Cr-Ni alloy — T. Suga · · · 577

85 Impact of inhomogeneity of nucleus upon δ-γ Massive-like transformation analyzed by phase field modeling — K. Kurotsu · · · 578

86 Cellular automaton simulation of solidification microstructures for Fe-C alloys considered a peritectic reaction — J. Ogawa · · · 579

87 Numerical simulation of nonequilibrium solidification without assuming stefan condition — K. Takahashi · · · 580

Continuous casting and solidification 1

88 Scale ratio and fluid properties for multiple non-dimensional numbers similitude of physical modeling for precise representation of flow phenomena — Y. Tsukaguchi · · · 581

89 Influence of mold level fluctuation on unevenness of solidified shell deformation in mold — K. Furumai · · · 582

90 Influence of manganese content on unevenness of initial solidified shell thickness — K. Watanabe · · · 583

91 Prediction and improvement of inner crack of continuous casting copper ingot — T. Sakamoto · · · 584

Continuous casting and solidification 2

92 Observation and analysis of segregation in laboratory-scale experiment of Sato mold using medium-carbon steel — J. Ma · · · 585

93 2-dimension center-line segregation simulation of continuous casting — T. Murao · · · 586

94 Macro-segregation observation and prediction in sand cast steel — A. Kishimoto · · · 587

95 (ISIJ Research Promotion Grant) Development technology for prevention of macro-segregation in casting of steel ingot by using insert casting — K. Isobe · · · 588

Continuous casting and solidification 3

96 withdraw

97 Effect of CaO substitution with BaO for development of fluorine-free mold fluxes — Z. Wang · · · 589

98 Carburizing behavior of steel by molten cast iron — Y. Nagashima · · · 590

Program of the 178th ISIJ Meeting (September 11-13, 2019)

Environmental, Energy and Social Engineering

Lecture No. / Plenary Session	Title	Speaker	Page
Advanced utilization of by-materials			
99	(ISIJ Research Promotion Grant) Recovery of phosphorus from steelmaking slag	M. Uchikoshi	591
100	Optimization of the high phosphate slag fertilizer (Report of the workshop on the effective application of phosphate in the steelmaking slag 1)	T. Harada	592
101	Trial to utilize phosphate in the steelmaking slag for plant cultivation (Report of the workshop on the effective application of phosphate in the steelmaking slag 2)	J. Wasaki	593
102	Long-term alkali elution from steelmaking slag filled in an open channel into seawater	Y. Matsuda	594
103	Fertilization effect of steelmaking slag granules on growth of nori	M. Takano	595
Eco-process and iron making			
104	Fabrication of iron oxide nanoparticles via submerged photosynthesis and the morphologies under different light sources	L. Zhang	596
105	(ISIJ Research Promotion Grant) Development of low flow rate cooling technology for a mold plate of continuous casting with uni-directional porous copper	K. Yuki	597
106	Thermal and mechanical durability of aluminized iron-based heat storage materials	S. Miura	598
107	Test of direct ironmaking process in the early Kofun period	K. Nishimura	599

Instrumentation, Control and System Engineering

Lecture No. / Plenary Session	Title	Speaker	Page
Instrumentation 1			
108	Inline evaluation of mechanical properties of steel sheets by electro-magnetic method	H. Yamada	600
109	Statistical evaluation method for material uniformity using ultrasonic scattering	T. Morinaga	601
110	The report on the research group of pipe wall measurements using the circumferential guided waves (11) (Study on the circumferential guided waves EMAT using resonance method)	R. Murayama	602
111	Evaluation of inspection properties for inclusions in steel by X-ray CT and UT	K. Ozaki	603
Instrumentation 2			
112	High-precision temperature measurement of materials in a heating furnace	M. Muramatsu	604
113	Measurement of slag emissions using blast furnace tap hole camera	K. Kuwana	605
114	Neural network model for predicting surface defects of wire rods	I. Son	606
Control and system			
115	Crossbow correction for uniform coating weight control	C. Jee	607
116	Operation guidance on thermal control of blast furnace	Y. Hashimoto	608
117	An optimization for ore yard operation schedules using multi-start greedy algorithm	A. Kumano	609
118	Applying column generation to stack sorting problem in the slab yard	T. Kurokawa	610

Processing for Quality Products

Lecture No. / Plenary Session	Title	Speaker	Page
Modeling of various phenomena in metal forming and its application 1			
119	Dislocation density base modelling of flow stress during tensile testing with holding/unloading and reloading in high tensile strength steel	N. Ueshima	611
120	Prediction of ductile fracture in upset forging by an ellipsoidal void model	K. Komori	612
121	Comparative simulations of hot deformation behavior under varying thermal-mechanical conditions	Y. Liu	613
Modeling of various phenomena in metal forming and its application 2			
122	Evaluation of cold forge solid phase bonding strength between carbon steel and pure aluminum	H. Nagata	614
123	Experimental verification of simplified identification method of yield function using circumscribing polygon	S. Kodama	615
124	Analysis of draw/re-draw process using Yld91 yield function and non-associated flow rule	A. Yoshimura	616
125	Elastic-plastic FEM analysis of tension leveling with different constitutive models	H. Wang	617

Program of the 178th ISIJ Meeting (September 11-13, 2019)

Reliability evaluation of steel weld 1

126 Construction of microstructural diagram for steel based on crystallography — K. Tsutsui · · · 618
127 Effect of metal vapor transport on electrode deformation during TIG welding — K. Tanaka · · · 619
128 Numerical simulation for consumption process of tungsten electrode during TIG welding — M. Tanaka · · · 620

Reliability evaluation of steel weld 2

129 Evaluation of ratio of lattice defects in multi-pass welds of reduced activation ferritic/martensitic steel F82H using positron annihilation technique — H. Mori · · · 621
130 Solidification evolution and the cracking susceptibility in weld metal of austenitic stainless steels — K. Kadoi · · · 622
131 Numerical simulation of effect of microstructure on hydrogen-related cracking of duplex stainless steel weld metal — Y. Mikami · · · 623

Control technology for free cutting-13

132 Influence of MnS aspect ratio on machinability of free-cutting ferritic stainless steel — M. Tojo · · · 624
133 (ISIJ Research Promotion Grant) Effect of shot grid diffused layer generated by hot shot peening on surface hot shortness — A. Takemura · · · 625
134 Cutting characteristic of Co-Cr-Mo alloy — M. Hagino · · · 626
135 Machinability of inconel material by ball end milling — T. Inoue · · · 627

The technical session by young engineers of hot rolling 1

136 The combustion control using the calorimeter — R. Shima · · · 628
137 Reduced of scale loss by optimization of air ratio in the reheating furnace at hot strip mill — S. Harada · · · 629
138 Reheating temperature reduction by the heat retention cover — T. Ushizawa · · · 630

The technical session by young engineers of hot rolling 2

139 Actions to improve strip passability in finishing mill — K. Nohgashira · · · 631
140 Inhibiting thermal elevation of finishing roll chock — T. Sasaki · · · 632
141 Improvement of strip thickness accuracy in hot strip — A. Okamatsu · · · 633

Young engineer's latest researches on tubes and pipes II-1

142 Improvement of formability in rotary draw bending for high strength steel tubes — S. Tamura · · · 634
143 FEM simulation of one-sided rubber bulging test of metal tube — K. Nakahara · · · 635
144 New cutting method of metal pipes with twist shearing — S. Kyuma · · · 636

Young engineer's latest researches on tubes and pipes II-2

145 Material modeling using multiaxial tube expansion tests and hole expansion forming simulation of hot-rolled steel sheet — S. Nomura · · · 637
146 Estimation of creep strain equation of weld metal and HAZ in Mod.9Cr-1Mo steel welded joint — T. Nakamura · · · 638
147 Fabrication of β titanium alloy microtubes using laser dieless drawing — T. Furushima · · · 639

Advances in processing of powders and powder metallurgy

148 Contact fatigue properties of sintered and rolled gear applied for Ni-Mo pre-alloy steel powder — Y. Taniguchi · · · 640
149 The relationship between dimensional accuracy and copper content variation during continuous compaction in iron-based sintered material — S. Unami · · · 641
150 Fabrication of micro parts by viscous flow processing of Pd metallic glassy particles — N. Yodoshi · · · 642
151 Effect of preheating under glass transition temperature on green density of ferrous metallic glass powders by viscous flow compaction — T. Kamogawa · · · 643

Scale and cooling

152 Analysis of factors affecting scale detachment of low carbon steels — D. Kim · · · 644
153 Effect of non-stoichiometry in $Fe_{1-x}O$ layer on thermal effusivity of oxide scale — R. Endo · · · 645
154 Boiling heat transfer characteristics of water jet to high-speed moving plate — T. Hirao · · · 646
155 Development of a computational model for water spray quenching of steel — H. Funagane · · · 647

Cooling

156 Controllability of the stopping temperature of fast cooling by hot compression testing machine — S. Ding · · · 648
157 Design of feedforward control system for 3-stage cooling based on simplified temperature distribution model for run out table of hot strip mill — R. Saito · · · 649
158 The effect of boiling regime on residual stress in steel sheet after spray cooling — S. Yanagi · · · 650

Hot rolling

159 Decoupling of effect of inter-roll thrust force on off-centering control based on differential force — K. Yamaguchi · · · 651
160 Efficiency improvement activity in Keihin — T. Koyama · · · 652
161 Examination of generation mechanism of Periodically changing telescope — T. Akashi · · · 653
162 An study on reducing lateral bulging deformation in width direction during hot plate rolling — Y. Jung · · · 654
163 Development of anti-grain coarsening low alloy steel for carburizing — W. Chiu · · · 655

Fundamental tribological studies on manufacturing processes

164 Sticking in hot rolled sheet of ferritic stainless steel — Y. Matsubara · · · 656
165 Development of air atomization supplying method in hot rolling process — T. Inoue · · · 657
166 Curling of hot rolled sheet due to scale on steel surface — R. Aizawa · · · 658
167 Shear mode fatigue crack propagation test for casting high carbon HSS roll material — N. Oda · · · 659
168 Evaluation of surface topology of rolled sheet by oils with different lubricity — Y. Okada · · · 660

Microstructure and Properties of Materials

Lecture No. / Plenary Session — Title — Speaker — Page

Modeling and simulation 1

169 Simulation of clustering process of solute atoms in BCC-Fe based on first principles calculation — M. Enoki · · · 661
170 First-principles calculations of solute atoms cluster of N and substitutional elements in α-Fe — T. Uesugi · · · 662
171 Fe-N potential using FS potential — K. Hyodo · · · 663
172 Numerical analysis of internal stress in pearlite by molecular dynamics and its comparison with elastic theory — Y. Amemiya · · · 664

Modeling and simulation 2

173 Thermodynamic assessment and calculations of the Fe-Cr-C phase diagrams — K. Oikawa · · · 665
174 Calculation of grain boundary segregation for boron and carbon based on thermodynamic analysis of the Fe-B-C ternary system — K. Takahashi · · · 666
175 Prediction of microstructure development of DP steel by quantitative phase-field method — N. Kiyokane · · · 667
176 Flow stress by inverse analysis with dynamic recovery and recrystallization model of duplex stainless steel — K. Kim · · · 668

Plate and machine structural steel

177 withdraw
178 Effect of primary rolling condition on microstructure and mechanical property of the steels after secondary rolling — R. Sakai · · · 669
179 Effects of forging temperature and concentrations of alloying elements on austenite grain structures during carburization of case-hardening steel — G. Saito · · · 670

Phase transformation

180 Modeling of the dynamic transformation above the Ae3 temperature — R. Shiraishi · · · 671
181 Effect of compressive stress on pearlite transformation in high carbon steel — R. Ueji · · · 672
182 Recrystallization and improvement of rigidity of super invar cast steel by martensitic reversion — N. Sakaguchi · · · 673
183 Austenite recrystallization mechanism induced by martensitic reversion in super invar alloy — R. Bao · · · 674

Aging and precipitation

184 Microstructure formation along the eutectoid type reaction path of δ-Fe→γ-Fe+Fe_2Ta in Fe-Cr-Ta ternary system — Z. Yuan · · · 675
185 Effect of cooling rate on dispersion state of hard particles and soft particles in ferritic steel — T. Mizuguchi · · · 676
186 The effect of alloying elements on the high temperature tempering behaviors of Fe-N martensitic steels — S. Young · · · 677

Program of the 178th ISIJ Meeting (September 11-13, 2019)

Microstructure formation 1

187 Effect of grain size of austenite on formation of retained austenite of low alloy TRIP steels — H. Hasegawa · · · 678

188 Characteristics of ferrite and the effect on the mechanical properties of cold rolled high strength steel with composite microstructure — T. Nakagaito · · · 679

189 Comparison of carbon content in retained austenite and martensite by combination of FE-EPMA and EBSD techniques — Y. Tanaka · · · 680

190 Microstructure observation of martensite in quenched medium-carbon low-alloy steel — T. Niho · · · 681

Microstructure formation 2

191 The effect of holding conditions after deformation on the transformation texture change of hot deformation material — Y. Takeuchi · · · 682

192 Visual analysis of local strain distribution with marker method for cold-rolled steel sheet — R. Kurosaka · · · 683

193 Heterogeneous nano-structures in stainless steels developed by heavy cold rolling and mechanical properties — H. Miura · · · 684

Hydrogen embrittlement 1

194 Standardization of mechanical testing in high-pressure hydrogen environment with a hollow specimen — T. Ogata · · · 685

195 Evaluation on the interaction between SUS304 steel and hydrogen gas by using hollow specimens — S. Kumagai · · · 686

196 A quantum chemical approach to hydrogen embrittleness — S. Kumagai · · · 687

Hydrogen embrittlement 2

197 Hydrogen embrittlement fracture behavior of a Ni-based superalloy 718 under internal and external hydrogen environments — Y. Ogawa · · · 688

198 Behavior of hydrogen in a SUS430J1L steel — T. Okazaki · · · 689

199 Effect of microstructure on hydrogen embrittlement of high strength Fe-Ni-Al-C Alloy — G. Amou · · · 690

Hydrogen embrittlement 3

200 Strain dependence of lattice defect formation enhanced by hydrogen in pure iron — Y. Sugiyama · · · 691

201 Local analysis near hydrogen embrittlement fracture surfaces of pipeline steel X80 with stress concentration — T. Homma · · · 692

202 Reduction of hydrogen embrittlement susceptibility in high strength steels through precipitated VC — K. Hokazono · · · 693

203 Hydrogen trapping states and hydrogen embrittlement susceptibility of high strength weld metal — R. Inoue · · · 694

Hydrogen embrittlement 4

204 Crack initiation and propagation analysis in hydrogen induced cracking of tempered martensitic steel — T. Chiba · · · 695

205 Lattice defect analysis near the initiation / propagation of hydrogen-induced cracking in tempered martensitic steel — T. Chiba · · · 696

206 Comparison of hydrogen desorption spectra and substructure of tempered martensitic steel applied to cyclic stress with/without hydrogen — M. Ohori · · · 697

207 Reduction in delayed fracture susceptibility of tempered martensitic steel — S. Hagiwara · · · 698

Hydrogen embrittlement 5

208 Comparison of fracture morphologies obtained by different methods of evaluating hydrogen embrittlement of multi-phase high strength steels — D. Asari · · · 699

209 Effects of test conditions on interactions between hydrogen and plastic deformation of high strength multi-phase steel sheet — K. Yashima · · · 700

210 Effect of pre-strain on the hydrogen embrittlement property in a TRIP-aided bainitic ferrite steel — B. Kumai · · · 701

211 Evaluation of hydrogen embrittlement of tempered martensitic steel by using U-bending — Y. Shibayama · · · 702

Stainless steels 1

212 Estimation of Young's modulus by the direct averaging method in isotropic polycrystalline austenitic steel — S. Takaki · · · 703

213 Effect of Young's modulus in single crystal on the elastic stiffness of austenitic steel — S. Takaki · · · 704

214 Age hardening behavior at low temperature in high-nitrogen austenitic stainless steel — K. Naridomi · · · 705

215 Influence of amount of austenite on tensile behavior for martensitic precipitation hardening stainless steels — R. Teko · · · 706

Stainless steels 2

216 Effect of applied stress on pitting corrosion at sulfide inclusions on Type 304 — S. Tokuda · · · 707

217 (ISIJ Research Promotion Grant) Application of stainless steels for alkaline water splitting electrodes — N. Todoroki · · · 708

218 Effect of Nickel and Nitrogen on pitting initiation of lean duplex stainless steel on heat affected zone — Y. Yonenaga · · · 709

Stainless steels 3

219 In-situ observation of the wetting process on stainless steel surface in atmosphere blazing — A. Kawano · · · 710
220 Surface film analysis and Cr vaporization property of bright annealed Al added 18%Cr stainless steel — M. Sugeoi · · · 711
221 Increase of Si content in 20Cr-5Al ferritic stainless steel by siliconizing process — A. Mizutani · · · 712
222 Effect of Ni addition on ductile-to-brittle transition temperature in 11Cr ferritic stainless steels — K. Inoue · · · 713
223 The relationship between intermetallic compounds precipitation and concentration profile of Cr in short-time aged duplex stainless steels — N. Nishizawa · · · 714

Strength and deformation behavior 1

224 Effects of C and N on Hall-Petch coefficient of austenitic stainless steel — Y. Oka · · · 715
225 Temperature dependence of grain refinement strengthening in SUS316L stainless steel — K. Tsugumi · · · 716
226 (ISIJ Research Promotion Grant) Low temperature tensile properties in aged ultra-low carbon ferritic steel — N. Koga · · · 717
227 Relationship between dislocation density and elastic limit in 0.3mass%-carbon martensitic steel — Y. Suzuki · · · 718

Strength and deformation behavior 2

228 An evaluation on strain rate sensitivity under mode I deformation in energy absorption characteristic of thin specimens made of SUS304 — S. Yoshida · · · 719
229 An evaluation of energy absorption in SUS304 by small punch test at 2 kinds of deflection rate — Q. Chen · · · 720
230 (ISIJ Research Promotion Grant) An evaluation on rate sensitivity of axial strength of joints using Fe-28Mn-6Si-5Cr shape memory alloy — T. Iwamoto · · · 721
231 Effect of high nitrogen austenite on tensile properties of nitrogen steel — K. Kikuchi · · · 722

Strength and deformation behavior 3

232 Understanding serration behavior in high-Mn austenitic steel from a view point of work hardening and plastic deformation — S. Hwang · · · 723
233 A finite element analysis on anomalous deformation behaviour in thin specimen made of SUS304 by considering dynamic strain aging — Y. Nishigaki · · · 724
234 An observation of anomalous deformation behavior during quasi-static tensile test in sheet specimen made of SUS304 — D. Tamura · · · 725

Strength and deformation behavior 4

235 Analysis of heterogeneous deformation behavior in austenitic stainless steel using high resolution digital image correlation method — S. Takahashi · · · 726
236 Hybrid analysis of deformation behavior of austenitic stainless steel — H. Yamada · · · 727
237 Effect of cementite morphology on local deformability in C-Mn eutectoid steels — T. Nagasako · · · 728

Strength and deformation behavior 5

238 Prediction of hole expansion ratio for various steel sheets based on uniaxial tensile properties — J. Kim · · · 729
239 Inhomogeneous deformation behavior of multi-phase steel subjected to tensile and compression periodic test — T. Morikawa · · · 730
240 A study on compressive deformation and shape recovery behavior of Fe-28Mn-6Si-5Cr shape memory alloy under cyclic thermo-mechanical loading — Q. Sun · · · 731
241 Cyclic tension-compression test for 590 MPa dual phase steel and its constitutive model — H. Nakamoto · · · 732

Electrical steel 1

242 Nitriding in strain release annealing — Y. Natori · · · 733
243 EBSD observation of pure iron with cube texture — D. Okai · · · 734
244 TEM observation of {411} <148> recrystallization behavior from α-fiber deformed grain in Fe-3%Si alloy — M. Yasuda · · · 735

Electrical steel 2

245 Influence of lubrication conditions on rolling texture in 3%Si steel — Y. Shimoyama · · · 736
246 Effect of cutting methods on cut-edge magnetic domain structures of 3% silicon steel — J. Hong · · · 737
247 (ISIJ Research Promotion Grant) Magnetic properties of non-oriented steel sheet under in-plane isotropic stress applied by piezoelectric element — S. Hashi · · · 738
248 (ISIJ Research Promotion Grant) Magnetic property analysis of over flux line in transformers — S. Ishikawa · · · 739

Program of the 178th ISIJ Meeting (September 11-13, 2019)

Recrystallization and grain growth 1

249 Solubility of In in austenite and influence of In on grain growth — J. Nakamura · · · 740
250 Recrystallization behavior of IF steel at the interface of Al junction — K. Okuda · · · 741
251 Relationship between three-dimensional microstructure and Avrami exponent for recrystallization in pure iron — T. Ogawa · · · 742
252 Effect of MnS particle on grain growth of ferrite — M. Seki · · · 743

Recrystallization and grain growth 2

253 Texture development of cold-rolled and annealed magnetostrictive Fe-Ga alloy — Y. Hayakawa · · · 744
254 Effects of Nb-addition and initial microstructures on microstructural evolution during annealing in low-carbon steel sheets — H. Dannoshita · · · 745
255 Abnormal grain growth in Nb-added case hardening steel during high temperature carburization — R. Tsuji · · · 746
256 In-situ observation of abnormal grain growth of austenite of case hardening steel — Y. Imanami · · · 747

Ferritic heat resistant steel 1

257 Influence of creep deformation behavior on creep life and rupture ductility of W-Mo-balanced 9Cr steel — F. Abe · · · 748
258 Non-destructive evaluation of segregation in ferritic creep resistant steel — K. Kimura · · · 749
259 Influence of segregation on creep strength of ASME Grade T91 steels — K. Kimura · · · 750
260 (ISIJ Research Promotion Grant) Microstructure evolution of a high boron 9%Cr heat resistant steels crept at 650 and 700 degree-C — N. Sekido · · · 751

Ferritic heat resistant steel 2

261 Interface failure assessment of dissimilar welded joints by circular notch specimen — H. Yamashita · · · 752
262 High temperature oxidation suppression mechanism in high nitrogen 9%Cr ferritic heat resistant steels — Y. Tonoe · · · 753
263 Development of low thermal-expansion and high creep-resistance ferritic heat resistant steels -Effects of alloying elements on thermal expansion of ferritic iron- — H. Fukunishi · · · 754
264 Creep rate estimation of 2.25Cr-1Mo steel by precipitates distribution analysis — H. Hayakawa · · · 755

Austenitic heat resistant steel and heat resistant alloy

265 Effect of Phosphorus and Niobium addition on creep strength of wrought Ni-based super alloy — Y. Hasebe · · · 756
266 Creep behavior of Ta added novel austenitic laves steels at 1073K — Y. Mitsuya · · · 757
267 Grain size dependence of creep in austenitic single phase steel — H. Wakabayashi · · · 758
268 Reproducing experimental study by computational study about TCP phase and GCP phase precipitation behavior in Fe-Cr-Ni-Nb austenitic heat-resistant steels — K. Kikuchi · · · 759
269 Phase equilibria among A1/TCP/*oP* in Ni-Cr-Mo ternary system at 973 K — R. Nagashima · · · 760

Fatigue property

270 10^{11}-cycle gigacycle fatigue tests on high-strength steel — Y. Furuya · · · 761
271 Giga-cycle fatigue properties of A5083P-O and A7075-T5 aluminum alloys — H. Hirukawa · · · 762
272 Investigation of fracture process in rotational bending fatigue test of soft nitrided JIS SCM420 steel — N. Ihara · · · 763
273 Fatigue life characteristics for low carbon steel with simulated HAZ heat treatments — H. Nishikawa · · · 764

Toughness and ductility

274 Dependency of CTOD toughness on cementite cracking and its modeling in martensitic steels — T. Namegawa · · · 765
275 Effects of Cr addition on the low temperature toughness in high manganese austenitic steels — D. Izumi · · · 766
276 (ISIJ Research Promotion Grant) Evaluation of fracture toughness affected by micro voids in ductile to brittle transition — T. Kagimura · · · 767
277 Effect of wire drawing on crack formation in tensile deformation of pearlite steel — T. Teshima · · · 768

Hot-dip coating

278 Hardness and compressive deformation property of Fe-Zn solid-solution — A. Sengoku · · · 769
279 Correlation of interfacial microstructure with adhesive bonding in galvannealed interstitial-free steel sheets — H. Park · · · 770
280 Research on the crater degeneration process of galvannealed interstitial-free steel sheets — Y. Jeong · · · 771
281 Effect of Al content on plastic deformability of hot-dip Zn-Al coatings — T. Mitsunobu · · · 772
282 In-situ SEM observation for fracture behavior of hot-dip Zn-Al-Mg alloy coating on steel sheets by bending deformation — H. Yokoi · · · 773

Chemical property

283 Microstructure change of intermetallic compound layer formed in hot-dip Al coated steel — K. Shinozuka · · · 774

284 (ISIJ Research Promotion Grant) Characterization of dissolution resistance of ferrous materials to molten aluminum alloys using pseudo binary phase diagrams — I. Goto · · · 775

285 Effect of aggregate in primer on blistering — S. Takaoka · · · 776

286 Hydrogen generation over porous CeO_2 supported Ru catalysts and the effect of Fe addition — C. Ueda · · · 777

Hydrogen embrittlement 6

287 Effect of alloying elements on hydrogen diffusion in iron — T. Omura · · · 778

288 Interaction between hydrogen and alloying elements in α iron — H. Sawada · · · 779

289 Calculation model of hydrogen diffusion coefficient in steel — D. Akahoshi · · · 780

290 Effect of chromium on hydrogen absorption behavior in iron — Y. Vanadia · · · 781

Hydrogen embrittlement 7

291 Effect of adherent $MgCl_2$ amount on hydrogen permeation of iron covered with the rust — Y. Wang · · · 782

292 Hydrogen entry into steel during rust removal by blast — M. Kawamori · · · 783

293 (ISIJ Research Promotion Grant) Influence of microscopic damage and hydrogen on tensile-shear strength of clinched joint — D. Sasaki · · · 784

Hydrogen embrittlement 8

294 Evaluation of hydrogen-related cracking in duplex stainless steel considering microscopic distribution of stress and diffusible hydrogen — Y. Mikami · · · 785

295 Prediction model for weld hydrogen cracking in high strength steel weld in terms of residual stress and hydrogen diffusion behavior — Y. Sato · · · 786

296 Pre-heat temperature effect on hydrogen transportation behavior for y-grooved weld joint based on α multiplication method considering the stability condition of numerical analysis — G. Ozeki · · · 787

Process Evaluation and Material Characterization

Lecture No. / Plenary Session — Title — Speaker — Page

Surface and state analysis

297 Effect of plasma generation method on the surface of SUS316 in plasma nitriding — K. Miura · · · 788

298 Visualization of Fe chemical state distribution in sintered ore by imaging XAFS — M. Takagaki · · · 789

299 Phase identification of microstructure of multiphase steel by SEM at extremely low landing energy — T. Aoyama · · · 790

Crystal structure analysis

300 In-situ observation of phase fraction and carbon diffusion in bainite transformation of Low-Alloyed TRIP steel by neutron diffraction — T. Hirano · · · 791

301 Movement of ferrite/austenite interface under cooling and distribution of alloying elements — T. Amino · · · 792

302 Effects of dislocation interactions and dislocation characteristics on work hardening — K. Nakagawa · · · 793

303 Comparison of dislocation contrast in steel obtained by using SEM-ECCI and TEM — T. Mori · · · 794

Elemental analysis 1

304 Detection of free magnesia in steelmaking slag after aging process — S. Imashuku · · · 795

305 Polarized continuous white X-rays produced by linear polarizer made from $Li_2B_4O_7$ — R. Tanaka · · · 796

306 (ISIJ Research Promotion Grant) Fundamental parameter method for ED-XRF — J. Kawai · · · 797

307 Research on the cohesive property of iron ore fines — W. Pan · · · 798

Elemental analysis 2

308 (ISIJ Research Promotion Grant) Distribution of alumina inclusion particles in ferritic stainless steels in scanning laser-induced breakdown spectrometry using 1-kHz Q-switched Nd:YAG laser — K. Wagatsuma · · · 799

309 Application of LIBS to sorting of aluminum materials and detection of the inclusion particles — Y. Fugane · · · 800

310 Glass bead sample pre-treatment for inductively coupled plasma-atomic emission spectrometric analysis of major components in blast furnace slag — K. Nakayama · · · 801

Program of the 178th ISIJ Meeting (September 11-13, 2019)

ISIJ and JIM Joint Sessions

Lecture No. Joint Session	Title	Speaker	Page
Titanium and its alloys 1			
J1	Synthesis of $TiCl_4$ by low-temperature chlorination of TiN	E. Ahmadi	802
J2	Evaporation behavior of solute elements in Ti-alloy melt	H. Mizukami	803
J3	Effect of reaction rate on state in upper space above bath surface in actual sponge titanium production vessel	Y. Inoue	804
J4	Manufacturing of high quality titanium thin foil of A4 size by electrodeposition route	Y. Nakajo	805
J5	Nanoscale analysis of cross-sectioned microstructure after machining in Ti531C alloy with Cu and Ni addition	T. Furuhara	806
Titanium and its alloys 2			
J6	Rapid oxidation and nitriding of additive manufactured Ti-6Al-4V alloy by induction heating in air	K. Tamura	807
J7	Comparison of pressformability in commercially pure titanium JIS class1 sheet and interstitial free steel sheet	R. Miyoshi	808
J8	Effect of interactions among grains on slip system activation and its range in αTi	Y. Kawano	809
J9	Effect of Al addition on tensile deformation property of Ti-18Nb-xAl alloys	Y. Mantani	810
J10	Effect of V on mechanical properties and age-hardening behavior of Ti-Mn alloys	Y. Nakamura	811
Titanium and its alloys 3			
J11	Dependence of microstructure on creep behavior and deformation mechanism in near-αTi alloy	H. Masuyama	812
J12	Constitutive plastic behavior, Dynamic globularization and machine learning of the Ti-6246 alloy under hot forging process	H. Matsumoto	813
J13	Formation of silicide of high-temperature near-α Ti alloys	Y. Yamabe-Mitarai	814
Titanium and its alloys 4			
J14	Effect of interstitial elements on hot deformation behavior and microstructure evolution of Ti-17 alloys	T. Tsukase	815
J15	Dynamic precipitation of alpha phase during deformation in Ti-17 alloy	E. Chandiran	816
J16	Effect of hot multi-directional compression on dynamic recrystallization in Ti-17 alloy	A. Ito	817
J17	Relationship between microstructure and mechanical properties of Ti-17 alloy for aerospace application and machine learning	D. Tadokoro	818
J18	Deformation-static recrystallization behavior of Ti-5553 alloy for aerospace application	M. Yoshimura	819
Ultrafine grained materials -fundamental aspects for ultrafine grained structures- 1			
J19	Relationship between nanostructure and mechanical properties of electrodeposited nanocrystalline nickel	T. Hayashi	820
J20	Effect of low temperature on deformation behaviors of Mg-0.1 at.%Y alloy having various grain sizes	K. Oki	821
J21	Influence of ECAP processing and heat treatment on tensile property and fatigue crack initiation in ZK60A magnesium alloy	K. Umeda	822
Ultrafine grained materials -fundamental aspects for ultrafine grained structures- 2			
J22	Microstructure and mechanical properties of fine-grained Ti-25Nb-25Zr alloy prepared from TiH_2 mixed elemental powders	B. Sharma	823
J23	Microstructure and mechanical properties of harmonic structure designed CrMnFeCoNi high entropy alloy	N. Togawa	824
J24	Peculiar mechanical properties and its mechanism of harmonic structured pure copper	M. Kawabata	825
Ultrafine grained materials -fundamental aspects for ultrafine grained structures- 3			
J25	Microstructure distribution through radius of pure aluminium rod deformed by surface shear extrusion	N. Kamikawa	826
J26	Effect of stacking fault energy on microstructural evolutions and mechanical properties of FCC metals processed by severe plastic deformation	M. Asano	827
J27	Nano-crystallization of quasi-stabilized austenitic stainless steels by dry ice particle peening	S. Minamimoto	828
Materials science of martensitic and bainitic transformations and its applications 1			
J28	Negative Poisson's ratio in single-crystal Cu-Al-Mn shape memory alloys	S. Xu	829
J29	Kinetic arrest of R-B19' transformation in Ti-(50-*x*)Ni-*x*Fe shape memory alloy	M. Todai	830

J30 Synchrotron radiation analysis on controlling mechanism of excellent strength and ductility in low carbon -2Si-5%Mn fresh martensitic steel — T. Fuse · · · 831

J31 Development of 1500MPa-30% high strength and high ductility 5% Mn ferrite+austenite steels and synchrotron radiation analysis on the mechanism to emerge the excellent mechanical properties — K. Minoda · · · 832

Materials science of martensitic and bainitic transformations and its applications 2

J32 Sensitivity coefficients of martensite microstructure to material parameters in steel — Y. Tsukada · · · 833

J33 Internal stress of hcp-martensite formed in Fe-Cr-Ni alloys — Y. Wada · · · 834

J34 Analysis of deformation behavior of martensite in a ultra-low carbon steel by crystal plasticity finite element method — S. Nambu · · · 835

J35 Segregation of boron to austenite grain boundary during cooling after high temperature austenitization — G. Miyamoto · · · 836

Materials science of martensitic and bainitic transformations and its applications 3

J36 Effect of thermo-mechanical control process on toughness of medium Mn martensitic steel — S. Okuhata · · · 837

J37 Martensitic transformation of high-entropy and medium-entropy alloys — H. Matsuda · · · 838

J38 Effect of the grain boundary a particle on martensite transformation behavior in Fe-Ni-Si alloys — K. Kitamura · · · 839

J39 Giant elastocaloric effect with wide temperature window in nanocrystalline Ti-44Ni-5Cu-1Al shape memory alloy — F. Xiao · · · 840

Materials science of martensitic and bainitic transformations and its applications 4

J40 Effects of peening direction on reverse transformation induced by shot-peening for Fe-Ni alloys — H. Sato · · · 841

J41 Effect of precipitates on dislocation-reducing rate in tempering treatment — S. Yoshida · · · 842

J42 The microstructure and mechanical properties of medium-Mn steels treated with interrupted quenching and intercritical annealing — S. Tanaka · · · 843

J43 Analysis of carbide chemical composition of Si-added middle carbon tempered martensitic steels — T. Suzuki · · · 844

Materials science of martensitic and bainitic transformations and its applications 5

J44 Room temperature aging behavior of low-to-medium carbon low alloy ferrous lath martensite — N. Maruyama · · · 845

J45 In-situ heating TEM study of carbides in low-carbon martensite — Y. Fukuo · · · 846

J46 Alloying effects on low-temperature tempering behaviors of high-carbon martensite — Y. Zhang · · · 847

J47 Visualization of hydrogen release from lath martensite transformed from hydrogen-charged austenite — K. Oie · · · 848

Materials science of martensitic and bainitic transformations and its applications 6

J48 Effect of tensile stress on the kinetics of isothermal martensitic transformation — W. Mao · · · 849

J49 Effects of prior austenite grain size on microstructure of bainite and retained austenite in TRIP steel — M. Watanabe · · · 850

J50 Microstructure and local orientation relationship of lower bainite in carbon steels — T. Hayashi · · · 851

Materials science of martensitic and bainitic transformations and its applications 7

J51 Invariant line analysis of experimental martensite orientation relationship — D. Akahoshi · · · 852

J52 Morphology and crystallography of martensite in equiatomic HfNi alloy — M. Matsuda · · · 853

J53 Microstructural analysis of lenticular martensites in Fe-Ni-C alloy based on Rank-1 connection — Y. Shinohara · · · 854

J54 Geometrical models and matrices for fine crystals at crossing hexagonal ε variants — T. Sawaguchi · · · 855

Materials science of martensitic and bainitic transformations and its applications 8

J55 Magnetic-field-induced martensitic transformation and its in situ observation in Fe–Mn–Ga shape memory alloys — X. Xu · · · 856

J56 In-situ measurement of surface relief induced by martensitic transformation — J. Inoue · · · 857

J57 Recrystallization texture control of Ti-4.5Al-3V-2Fe-2Mo alloy — H. Tobe · · · 858

J58 Characterisation of the martensite blocks in Fe-C low alloy lath martensite — S. Morito · · · 859

Physico-chemical properties of high temperature melts 1

J59 Thermophysical property measurements of high temperature oxide melts using an electrostatic levitation furnace onboard the International Space Station - report 3 — T. Ishikawa · · · 860

J60 Excess volume and partial molar volume of Ti-X(X=Cu, Ni) melts — M. Watanabe · · · 861

J61 Measurement of apparent thermal conductivity of mould flux containing iron oxide by parallel plate method — T. Yamauchi · · · 862

J62 Examination of sample diameter for thermophysical property measurement of solid sample using surface heating and surface detection laser flash method — K. Mori · · · 863

Physico-chemical properties of high temperature melts 2

J63 Interfacial reaction and joining of Bi-Te materials against metallic substrates — S. Sukenaga · · · 864

J64 Wettability of Y_2O_3-SiO_2 composites with different SiO_2 activities against molten iron-based alloys — Z. Zhang · · · 865

J65 In-situ observation of the formation process of surface fine crevice structure by high-speed camera under laser-irradiation — J. Yeon · · · 866

J66 Measurement of speed of super-spread wetting on surface fine crevice structure by laser-irradiation — M. Nakamoto · · · 867

Physico-chemical properties of high temperature melts 3

J67 Wide-range composition dependence of viscosity of molten SiO_2-Na_2O-NaF system — O. Takeda · · · 868

J68 Influence of dispersed bubbles on viscosity behavior of triple phases coexisting slag — Y. Egashira · · · 869

J69 Thermodynamic properties of Sm-O system for high coercivity magnet material development — R. Nakazawa · · · 870

J70 Assessment of Cu behavior between Cu-containing multi-component slag and matte using the reaction model and measurement of Cu_2O activity coefficient — S. Shin · · · 871

Physico-chemical properties of high temperature melts 4

J71 Spontaneous colloidal metal cellular convection formation driven by molten salt electrolysis — S. Natsui · · · 872

J72 Thermal behavior of electrodeposited melt in molten salt electrolysis — R. Shibuya · · · 873

J73 Identification of solid phase in slag suspension by alternating current impedance method — Y. Takao · · · 874

Physico-chemical properties of high temperature melts 5

J74 Proposal to determination method of density of oxide scale formed on steel — S. Shinohara · · · 875

J75 Crystal structure stability of Ca_2SiO_4-based solid solution predicted by Ab initio calculation — M. Suzuki · · · 876

J76 In-situ phase identification of crystal precipitated from molten CaO-SiO_2-P_2O_5-FeO slag — H. Serizawa · · · 877